Biophysical Journal, Volume *121*

Supplemental information

Mechanics of inactive swelling and bursting of porate pollen grains

Anže Božič and Antonio Šiber

SUPPORTING MATERIAL:
Mechanics of inactive swelling and bursting of porate pollen grains

Anže Božič
Department of Theoretical Physics, Jožef Stefan Institute, Jamova 39, 1000 Ljubljana, Slovenia

Antonio Šiber
Institute of Physics, Bijenička cesta 46, 10000 Zagreb, Croatia[*]
(Dated: January 13, 2022)

GENERATING CROSS-SECTIONAL PROJECTIONS OF MODEL POLLEN GRAINS

In Figs. 2 and 3 in the main text we show cross-sectional projections of the pollen grains. These are 2D projections of a 3D shape obtained by assuming rotational symmetry of the shape around the axis going through the geometric center of the shape and the pole of the pore. In the case of a single pore, the shape is indeed symmetric around this axis to an excellent accuracy, which can also be seen from the cross-sectional projections. The data shown in the figures was obtained by binning the face centers in 800 (2×400) angular intervals and calculating the average 2D-projected, cross-sectional coordinates in each of the intervals. The origin for such angular representation was positioned on the symmetry axis, at the point where the vertical line in the plots separates the pore from the exine. Such a procedure produces a set of data suitable for graphic representation.

ANALYTICAL APPROXIMATIONS FOR CRITICAL VOLUME AT BURSTING TRANSITION

A monoporate pollen grain with a relative additional volume v can be approximated as a union of two spherical caps: the first of radius R_{ex} representing the exine part of the grain, and the second of radius R_p representing the pore. Initially, $R_p = R_e$, but as v increases and the pore inflates, R_p continuously decreases all the way until the pore assumes the shape of a hemisphere, where R_p is the smallest. After this point, any further inflation of the pore requires an increase in R_p.

The internal pressure in the grain p is counteracted by the forces in the pollen wall. Examination of the force equilibrium in the two poles of the grain (one in the pore and the other in the exine) when the pore has a hemispherical shape yields

$$\frac{2T_p}{R_p} = \frac{2T_{ex}}{R_{ex}} = p, \tag{S1}$$

where T_p and T_{ex} are the tension stresses in the pore and the exine, respectively [1]. In the hemispherical state of the pore, we have $R_p = R_{ex}\theta_0$ and consequently $T_{ex} = T_p/\theta_0$. If the dominant contribution to the tension forces comes from the stretching part of the two-dimensional (2D) elastic energy, the stretching stresses T are proportional to strains ϵ, which gives

$$\epsilon_{ex} = \frac{f}{\theta_0}\,\epsilon_p, \tag{S2}$$

where we have accounted for the fact that the 2D stretching modulus of the pore is softer by a factor of f with respect to the corresponding 2D stretching modulus of the exine. The stretching strains can be obtained by examining the distances between the two points in the wall in the stress-free state of the grain and the corresponding distances in the inflated state of the grain, which gives

$$\begin{aligned} \epsilon_{ex} &= \frac{R_{ex}}{R_0} - 1, \\ \epsilon_p &= \frac{R_{ex}}{R_0}\,\frac{\pi}{2} - 1. \end{aligned} \tag{S3}$$

[*] asiber@ifs.hr

When $\theta_0 \ll 1$, the relative additional volume of the pollen grain with a hemispherical pore is given by

$$v_c = \left(\frac{R_{ex}}{R_0}\right)^3 \left(1 + \frac{\theta_0^3}{2}\right) - 1. \tag{S4}$$

From Eqs. (S2) and (S3), we have

$$\frac{R_{ex}}{R_0} = \frac{\theta_0 - f}{\theta_0 - f\pi/2}, \tag{S5}$$

and inserting Eq. (S5) into Eq. (S4), we obtain Eq. (6) in the main text. For a typical pollen grain, $f/\theta_0 \ll 1$ and $\theta_0 \ll 1$, and in this limit we further obtain Eq. (7) in the main text.

This derivation is only an approximation and is limited in scope. Equation (6) predicts that the bursting transition occurs only if $\theta_0 > f\pi/2$, as $v_c \to \infty$ when $\theta_0 = f\pi/2$. This is mostly satisfied by pollen grains, but it should be noted that the increase in volume in some pollen grains at bursting is comparable to the volume of a fully hydrated grain, $v \sim 1$. Furthermore, in the analytical derivation, the characteristic curvatures are assumed to be sphere-like, i.e., identical in the two principal directions both in the exine and in the pore. Numerically determined shapes do not have this property, although the principal curvatures do not differ much. The role of the neck region where the pore contacts the exine is also neglected in the approximation, even though it influences the curvatures of the grain shape, even in the polar region of the pore. This is particularly important for larger values of the softness parameter when the approximation of sphere-like curvatures becomes less accurate.

Validity of analytical approximations for bursting transition

While the numerical results presented in the main text mostly account for the geometry and elastic inhomogeneity which are to be expected in porate pollen grains (parameters θ_0 and f), it is of interest to examine the bursting transition for a wider range of parameters, since the bursting transition should vanish once the pore becomes hard enough. This will certainly be the case when $f = 1$ and the grain becomes effectively inaperturate, with $v_c \to \infty$. The analytical model in Eq. (6), however, predicts a divergence of v_c when $f = 2\theta_0/\pi$. In Fig. S1, we show how v_c changes as a function of f for a fixed $\theta_0 = 0.15$. Though large values of f (i.e., $f > 0.05$) are not expected to be typical for pollen grains [2, 3], the investigation of grains with larger f is nevertheless important in the more general context of the mechanics of soft pore inflation. The results indicate that the analytical approximation serves as a reasonably accurate guideline when $v_c < 0.8$, which is a situation typically encountered in pollen swelling and bursting. The approximations become significantly less reliable when $v_c > 1$. Somewhat fortuitously, the functional dependence in Eq. (7) can be used as a lower bound estimate for all the volumes v_c studied.

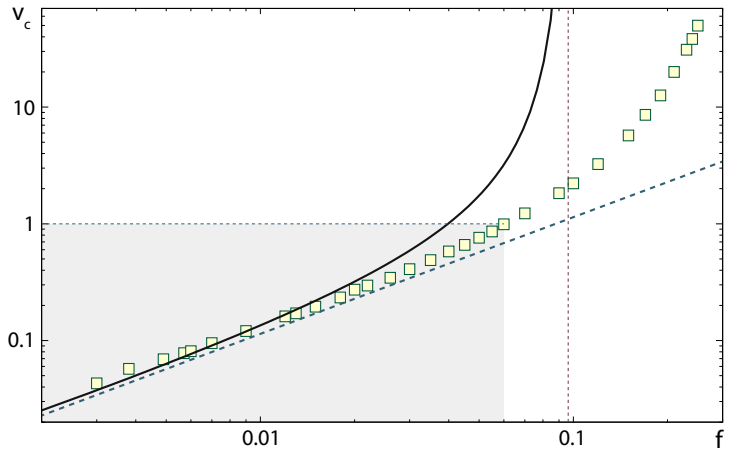

Figure S1. Critical volume at bursting transition v_c for a monoporate pollen grain with $\theta_0 = 0.15$ and $\overline{\gamma} = 10^4$ as a function of the pore softness parameter f. Numerically obtained results are denoted by symbols. Full and dashed lines are the predictions of Eq. (6) and Eq. (7) in the main text, respectively. The thin vertical dashed line indicates the value of f where the analytical expression in Eq. (6) diverges, $f = 2\theta_0/\pi$. The gray area of the plot indicates the range of (f, v_c) parameter space relevant to most pollen grains.

INTERNAL PRESSURE AND BURSTING TRANSITION

The calculations in the main text were performed for a given relative additional volume of the grain v. To each of the grain states obtained with the volume constraint one can also attribute an internal pressure P. The internal pressure can be obtained from the normal forces acting on the vertices of the shell in the absence of the volume constraint [4]. Figure S2 shows how the internal pressure in the pollen grain changes as its volume increases—this calculation is performed for the same set of parameters as those used in Fig. 2 in the main text. A sufficient pressure, denoted by P_c in Fig. S2, is required to overcome the energy barrier for bursting and the pressure drops once the pore inflates. This is similar to the phenomena observed in the inflation of a circular membrane [5] and rubber balloons [6, 7]. Comparing these results with those obtained by Božič and Šiber [4] for thin homogeneous spherical shells, we observe that the values of pressure are quite similar at a given increase of volume or exine radius. The pore decreases the pressure in the grain below the pressure which would act in an inaperturate grain at the same relative additional volume. This is indicated by the dashed line in Fig. S2, which shows the pressure obtained in the analytical limit of the microscopic model in Eq. (1) in the main text for an inaperturate grain with the stretching contribution only, $P = 2k_{ex}/(\sqrt{3}R_0)\, v$ [4].

We have also performed elastic energy minimization at a fixed internal pressure instead of the grain volume. In this case, the energy functional is augmented by an addition of a term PV [4, 8], and the volume constraint is released—this approach can be of interest when grain swelling is studied in solutions with different concentrations of non-metabolic sugars [9]. The calculations perfectly reproduce the critical volumes obtained in the fixed volume calculations, but the shapes obtained after the bursting transition (for $P > P_c$) have very large volumes and are difficult to stabilize in the minimization procedure. The large volumes of these shapes could also have been guessed on the basis of the nature of the pressure dependence in Fig. S2—the pressure *decreases* for $v > v_c$, which means that it can eventually return to its critical value of P_c only for large values of relative additional volume v. The bursting transition thus figures much more prominently in the calculations at a fixed internal pressure, although the grain shapes after the transition are difficult to obtain. Both approaches strongly corroborate the necessity of bursting (rupture) of the pore at $P = P_c$ or $v = v_c$ ($P_c = 0.232\ k/R_0$ and $v_c = 0.26$ for the case shown in Fig. S2 and Fig. 2, respectively).

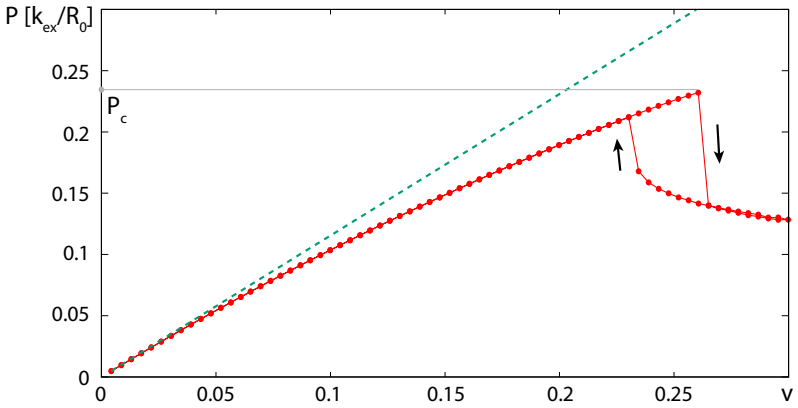

Figure S2. Internal pressure in the grain P as a function of the relative additional volume v. The pressure is shown in reduced dimensionless units of k_{ex}/R_0. Numerically obtained results are denoted by symbols. The dashed line shows the pressure obtained in the analytical limit of the microscopic model for the homogeneous inaperturate shell with stretching energy contribution only, $P = 2k_{ex}/(\sqrt{3}R_0)\, v$. The forward and backward minimization paths are indicated by arrows. The parameters of the calculation are the same as in Fig. 2 in the main text, $f = 0.02$, $\theta_0 = 0.15$, and $\overline{\gamma} = 10^4$.

INFLUENCE OF BENDING ENERGY ON BURSTING TRANSITION

All the results shown in the main text are calculated for $\overline{\gamma} = 10^4$. The range of $\overline{\gamma}$ typical for pollen grains was estimated by Božič and Šiber [2] to be between 3000 and 10000. This interval of $\overline{\gamma}$ was obtained by requiring that the colpate grains close regularly and completely as they dry up, and might not be entirely relevant for porate grains studied in this work. It is of interest to examine how different values of $\overline{\gamma}$ influence the bursting transition. Figure S3 shows how the critical volume at the bursting transition depends on the pore opening angle for three different values of $\overline{\gamma}$; smaller values of $\overline{\gamma}$ indicate a larger contribution of the bending energy. Figure S3 demonstrates that although

the bending energy influences the critical volumes (and pressures), the influence is relatively small and the results obtained in the main text for $\overline{\gamma} = 10^4$ can be considered to be representative for pollen grains. The bursting transition is smoother for smaller $\overline{\gamma}$, so that the full expansion of the pore occurs in a wider interval of volume.

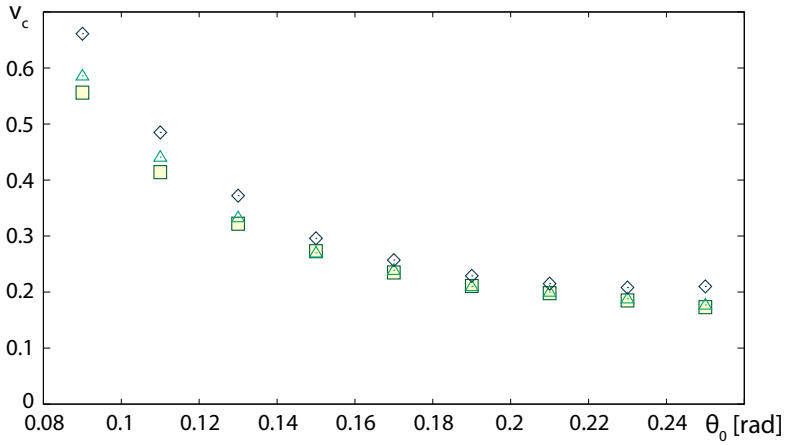

Figure S3. Critical volume at bursting transition v_c as a function of the pore opening angle θ_0 for $\overline{\gamma} = 10^4$ (squares), 5×10^3 (triangles), and 10^3 (diamonds). The pore softness parameter is $f = 0.02$.

NONLINEAR STRESS-STRAIN DEPENDENCE AND (NON-)UNIVERSALITY OF BURSTING TRANSITION

The calculated strains in the pore can become huge at the bursting transition. For instance, in the example in Fig. 2, the maximal extensional strain of the pore material *at* the bursting transition is 2.6. Such huge strains may require a modification of the Hookean stress-strain relationship employed in our simulations (see Materials and Methods in the main text). While such modifications can in principle be included in our model by allowing the elastic constants to vary with the local strain, in the situation where the elastic responses of the exine and the intine are poorly known such an undertaking does not appear to be particularly enlightening. Nevertheless, it is important to examine the robustness of the predicted bursting transition and investigate whether it persists in different elastic models of the pollen grain. To this end, we modified the stretching part of the Hookean elastic energy [Eq. (1)] to read

$$E_{stretch} = \sum_i \frac{k_i l_{i,0}^2}{2} \left| \frac{l_i}{l_{i,0}} - 1 \right|^p , \tag{S6}$$

where p is a real number, and performed calculations analogous to those shown in Fig. 2 (which correspond to the Hookean elasticity where $p = 2$). The formulation in Eq. (S6) has the advantage that the microscopic stretching and bending elastic constants of the edges k_i and ρ_i are kept the same for all p and have the same units as in the Hookean case. The stretching energies of the Hookean case and the p-power stretching elasticity coincide in an edge of length $l_i/l_{i,0} = 2$.

The pore bursting transition survives also in the more general parametrization of the stretching energy of Eq. (S6) for a range of values of p. There are, however, some differences from the Hookean case with $p = 2$. In particular, while the pores are visibly bulged out at the bursting transition for all powers p studied, the shape of the pore at the transition point is inflated a bit over the hemispherical shape when $p > 2$. Furthermore, the critical volumes of the transition sensitively depend on the power p, as demonstrated in Fig. S4. For $p > 2.4$, $v_c \gtrsim 1$ and the calculations become somewhat irrelevant for most porate grains as they do not tend to swell to such a high degree. It is also possible that for sufficiently large p, the bursting transition becomes completely suppressed and never takes place even for infinite increase in volume. This means that the aperture does not importantly modify the strains in the exine and that the entire grain swells almost as if it were inaperturate; this time not because the pore would be too small but due to the high power p in the nonlinear stress-strain relationship. A somewhat similar effect has been noted in relation to the blowout phenomenon of circular membranes and spherical patches, which takes place only for sufficiently small powers p in the energy functional of the problem [5]. A faithful modelling of pollen grain elasticity would require different parametrizations of the elasticity of the exine and the pores, in a much more involved manner

than using a simple scaling through a softness constant f. This is particularly relevant for large extensions of the exine and the pores, which are likely to be governed by quite different energy functionals and by an effective superposition of several power laws with different values of p [10].

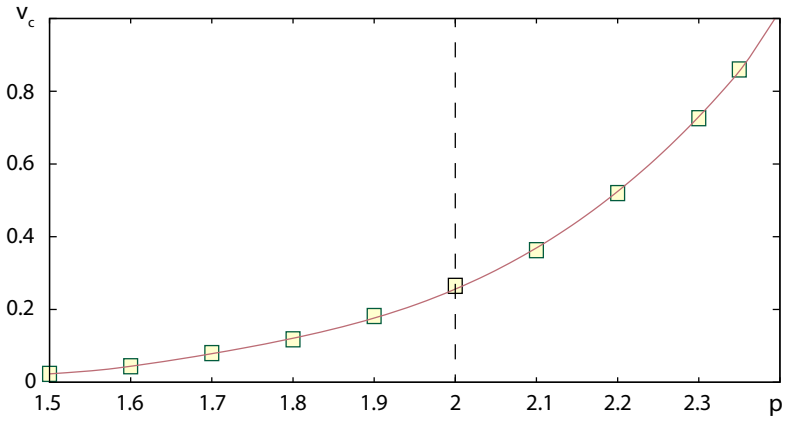

Figure S4. Critical volume v_c at which a pore rapidly inflates as a function of the power p in the parametrization of the stretching energy in Eq. (S6). Dashed vertical line emphasizes the point with $p = 2$ (Hookean dependence). The full line is a guide to the eye. The parameters of the elasticity of the monoporate grain are $f = 0.02$, $\theta_0 = 0.15$, and $\overline{\gamma} = 10^4$.

CODE AVAILABILITY

The computational code used to obtain the numerical results in the manuscript and the files pertaining to it (input files and the README file with the instructions required to reproduce the calculations) are publicly available in their entirety through the Open Science Framework (OSF): `https://osf.io/4q9ya/` [11].

[1] A. Šiber and P. Ziherl, *Cellular Patterns* (CRC Press, Taylor & Francis Group, Boca Raton, 2017).
[2] A. Božič and A. Šiber, Mechanical design of apertures and the infolding of pollen grain, Proc. Natl. Acad. Sci. USA **117**, 26600 (2020).
[3] E. Katifori, S. Alben, E. Cerda, D. R. Nelson, and J. Dumais, Foldable structures and the natural design of pollen grains, Proc. Natl. Acad. Sci. USA **107**, 7635 (2010).
[4] A. L. Božič and A. Šiber, Electrostatics-driven inflation of elastic icosahedral shells as a model for swelling of viruses, Biophys. J. **115**, 822 (2018).
[5] D. K. Bogen and T. A. McMahon, Do cardiac aneurysms blow out?, Biophys. J. **27**, 301 (1979).
[6] H. Alexander, Tensile instability of initially spherical balloons, Int. J. Eng. Sci. **9**, 151 (1971).
[7] A. Needleman, Inflation of spherical rubber balloons, Int. J. Solids Structures. **13**, 409 (1977).
[8] A. Šiber, Buckling transition in icosahedral shells subjected to volume conservation constraint and pressure: Relations to virus maturation, Phys. Rev. E **73**, 061915 (2006).
[9] A. Matamoro-Vidal, C. Raquin, F. Brisset, H. Colas, c. B. Iza, B. Albert, and P.-H. Gouyon, Links between morphology and function of the pollen wall: An experimental approach, Bot. J. Linn. Soc. **180**, 478 (2016).
[10] R. Ogden, Large deformation isotropic elasticity – on the correlation of theory and experiment for incompressible rubberlike solids, Proc. R. Soc. Lond. A **326**, 565 (1972).
[11] A. Šiber and A. Božič, Swelling of porate pollen grains (2022), OSF, 12 Jan. 2022. `https://osf.io/4q9ya`.